Smart Structures and Systems, *Vol. 30, No. 6 (2022) 649-659*
https://doi.org/10.12989/sss.2022.30.6.649

Dynamic deformation measurement in structural inspections by Augmented Reality technology

Jiaqi Xu [1a], Elijah Wyckoff [2b], John-Wesley Hanson [1c], Derek Doyle [3] and Fernando Moreu[*1]

[1] *Department of Civil, Construction & Environmental Engineering, University of New Mexico, Albuquerque, NM, USA*
[2] *Department of Mechanical Engineering, University of New Mexico, Albuquerque, NM, USA*
[3] *Air Force Research Laboratory, Space Vehicles Directorate, Kirtland Air Force Base, Albuquerque, NM, USA*

(*Received June 24, 2022, Revised August 29, 2022, Accepted October 29, 2022*)

Abstract. Structural Health Monitoring (SHM) researchers have identified Augmented Reality (AR) as a new technology that can assist inspections. Post-seismic structural inspections are conducted to evaluate the safety level of the damaged structures. Quantification of nearby structural changes over short-term and long-term periods can provide building inspectors with information to improve their safety. This paper proposes a Time Machine Measure (TMM) application based on an Augmented Reality (AR) Head-Mounted-Device (HMD) platform. The primary function of TMM is to restore the saved meshes of a past environment and overlay them onto the real environment so that inspectors can intuitively measure dynamic structural deformation and other environmental movements. The proposed TMM application was verified by demo experiments simulating a real inspection environment.

Keywords: augmented reality; deformation measurement; inspection; structural health monitoring; virtual images

1. Introduction

After severe earthquakes, buildings commonly undertake varying levels of damage (Sony *et al*. 2019). Deformation is usually used as the indices for quantifying numerically the damage in the buildings sustained under earthquake loading (You *et al*. 2022). Proper structural inspections are necessary to provide economic renovation and repair for the damaged buildings. Deformation measurement is one of the most important procedures in a post-seismic structural inspection.

Post-seismic deformation measurement mainly includes the structural deformation measurement and the overall deformation measurement (Mandler *et al*. 2021, He *et al*. 2022). Structural deformation measurement includes deflection measurement of horizontal members, verticality measurement of vertical members, and deformation measurement of nodes (Shan *et al*. 2016). To measure the deflection of horizontal members instruments such as leveling and laser, rangefinders are used, and for vertical members instruments such as theodolites, laser rangefinders, and total electronic stations are used (Sahu 2021). The deformation measurement of connecting nodes is usually directly measured and recorded with a tape measure and caliper instruments.

Instruments such as tape and caliper require inspectors to directly step into a damaged building, which will cause safety issues in a post-seismic situation. Instruments such as laser distance meter, theodolite, and total electronic station, can be conducted at a distance (Burachek *et al*. 2022, Lim *et al*. 2021, Rick 2018). However, the measurement time to conduct these instruments is relatively longer considering the complex operations. Because structural deformation is still in a dynamic procedure during the post-seismic inspections (Jin and Fialko 2021, Diao *et al*. 2021), a more straightforward and faster measurement method is required for the inspectors. Also, for safety reasons, inspectors should not get close to the damaged structures. Therefore, a measurement method dealing with dynamic deformation and conducted at a distance is necessary.

Today's solutions to measure structural deformation during the inspection process include comparing the current building visually with the embedded blueprint and recognizing the discrepancies (Kamat and El-Tawil 2005, 2007). Hazard reduction by identifying damage to individual structures in post-earthquake inspections is of great importance (Yekrangnia *et al*. 2021). Under the premise of enough time and access to the design blueprint, today's solutions work well for inspectors to quickly conduct a building safety assessment if they plan to enter a structure. However, the solutions today depend on the use of precise BIM models, which is always not available for a have-been-built structure. Therefore, in this paper, we use immediate 3D modeling to make it work independently of pre-built BIM models.

Zoellner *et al*. (2008) first described the 'time machine' concept in the Reality Filtering application. The Reality Filtering application is designed for cultural heritage

*Corresponding author, Ph.D., Professor,
E-mail: fmoreu@unm.edu
[a] Postdoctoral Researcher
[b] Masters Student
[c] Research Associate
[d] Associate Professor

ISSN: 1738-1584 (Print), 1738-1991 (Online)

projects, but the time machine idea is of great significance for engineering. Holmgren *et al*. (2014) designed a web-based prototype using the time machine concept. However, both apps are based on the PC or smartphone platforms, not fully used the advantages of AR devices.

This paper summarizes the design, development, and validation of Time Machine Measure (TMM), a novel tool to measure and share reference-free changes during an inspection. TMM can capture and measure changes in environmental movements and position over time and can assist inspectors by informing them of these changes over short and extended periods. Microsoft Hololens 2 HMD is controlled with hand gestures without the need for joysticks or external controllers, which is an advantage for field applications. No prerequisite for implementing the pre-input of the CAD model is needed in the TMM application. In the following sections, the authors first state the design theory, then summarize the AR software framework design, and finally present the human-device interface and operational instructions. The proposed TMM is first tested in a real indoor house for validation, as well as to identify further needs of programming and development for complex environments, with recommendations for future real-disaster scene implementation.

2. Measurement during inspection

Damage patterns have varying levels of seismic vulnerability, and the various damage patterns observed in built environments are first systematically classified by Shigeyuki and Takai (2000). For example, structural deformation consisting of inter-story drift and rigid body rotation can indicate progressive decay in the structure's stability (Lu *et al*. 2017). It would be valuable to distinguish structural deformation across time and other local movements, such as an inspection of a post-earthquake residential building. The structural deformation occurs during inspection can inform inspectors of real-time and short-term changes in their surroundings and help them classify damage and monitor changes over an extended period.

Today's solutions do not enable direct observation of the structural changes across time. Fig. 1 illustrates a straightforward example of the value of measuring structural deformation after a seismic event. In Fig. 1, d_1 represents the deformation exists before the disaster, including the initial construction error and rigid body rotation, which are informative but do not capture changes as time progresses. Conversely, d_2 represents the changes that can occur after the disaster. Current devices can only measure d_1 while a measuring method of d_2 is still not available today.

The authors design two primary functions to fulfill the core requirement of direct measurement of d_2: (i) time machine and (ii) measure. The time machine function enables inspectors to recreate structures recorded as a 3D mesh and overlay the past mesh in the present to track deformation across time. The measure function allows inspectors to measure the distance between past and present surroundings, i.e., measurement across time.

(a) Measure structural deformation (b) Real-time deformation d_2

Fig. 1 Schematic diagram of the structural deformation and inspection

3. AR device selection

The factors to be considered in selecting any AR platform consist of five fundamental categories: general properties, sensors, computational capabilities, connectivity, and display capabilities. Xu *et al*. (2022) summarized the parameters in each category. General properties include release date, country, weight, price, and product durability (waterproof, working temperature, relative humidity, and drop safe distance). Sensors consist of camera resolution, head-tracking sensor, eye-tracking sensor, depth sensor, gyroscope, accelerometer, magnetometer, and location sensor (GPS/GLONASS/GALILEO). Computational capabilities include the processing unit, Random Access Memory (RAM), and storage. Connectivity capabilities include WiFi, Bluetooth, USB, and battery capacity. Display capabilities include the field of view (FoV), Optics method, resolution, and refresh rate. An evaluation system can simplify the selection procedure of the AR platform. The composite score of an AR device, S, can be described as

$$S = v_i \sum_{i=1}^{m} w_i P_i \tag{1}$$

where P_i represents the i^{th} parameter considered in the selection. P_i can be a complete set or subset of all the parameters illustrated by Xu *et al*. (2022). Extra parameters can be added as demand in a specific implementation: w_i is the weighting coefficient of P_i, measuring the importance of the i^{th} parameter; v_i is the correction coefficient with values of $\{0 \quad 1\}$. If P_i is a necessary parameter for a specific application, then $v_i = 1$ for the devices with this character. Otherwise, $v_i = 0$.

The authors select the AR platform for inspection from the sixteen AR devices published in the last three years, with subset parameters provided by Xu *et al*. (2022). The weight and price of AR devices will decrease while increasing their outdoor durability, further augmenting the likelihood of field implementations. The authors use a correction coefficient for the depth sensor to meet the time machine function requirement and the inspection requirements. The weighting coefficient w_i of the device with the best behavior in this parameter is 1, and w_i of the other devices are multiplied with a fraction of P_i/P_{best}. For example, the Toshiba dynaEdge AR100 has a maximum working temperature of 60℃. Therefore, $w_{\text{temp}}(\text{Toshiba}) = 1$. The maximum working temperature of Google Glass Enterprise Edition 2 is 45℃. Therefore, $w_{\text{temp}}(\text{Google}) =$

Table 1 Evaluation score of AR devices for structural inspections

#	*Device*	*Depth Sensor* $v_i = 1\|0$	*Working Temperature* $w_i = 1.0$	*Camera 1.0*	*RAM 0.8*	*Storage 0.8*	*Battery 1.0*	*FoV 1.0*	*Weight 0.5*	*Price 0.5*	*Score*
1	Microsoft (2019)	1	0.45	0.50	0.50	0.50	1.00	0.65	0.08	0.14	**3.51**
2	Magic Leap 1 (2018)	1	0.42	0.31	1.00	1.00	0.01	0.63	0.15	0.22	3.14
3	ThirdEye Gen X2 Mixed Reality Smart Glasses (2019)	1	0.42	0.81	0.50	0.50	0.11	0.53	0.17	0.26	2.87
4	Toshiba DynaEdge AR100 Head Mounted Display (2018)	1	1.00	0.31	0.00	0.00	0.06	0.59	0.98	0.17	2.54
5	DAQRI Smart Glasses (2017)	1	0.42	0.50	0.13	0.50	0.35	0.38	0.14	0.10	2.26
6	Epson Moverio Pro BT-2200 Smart Headset (2017b)	1	0.67	0.31	0.13	0.06	0.08	0.29	0.15	0.25	1.69
7	Vuzix M400 Version 1.1.4 (2020)	0	0.75	0.50	0.75	0.50	0.01	0.21	0.54	0.28	0.00
8	Glass Enterprise Edition 2 (2019)	0	0.75	0.50	0.38	0.25	0.05	1.00	1.00	0.50	0.00
9	Kopin Golden-I Infinity Smart Screen (Carbotte 2018)	0	0.42	0.81	0.00	0.00	0.19	0.26	1.00	0.56	0.00
10	RealWear HMT-1Z1 (2018)	0	0.83	1.00	0.25	0.13	0.21	0.25	0.11	0.08	0.00
11	Kopin Solos Smart Glasses (Carbotte, 2018)	0	0.42	0.31	0.00	0.00	0.10	0.13	0.71	1.00	0.00
12	Everysight Raptor (2017)	0	0.67	0.81	0.25	0.25	0.13	0.94	0.47	0.77	0.00
13	Epson Moverio BT-350 Smart Glasses (2017a)	0	0.58	0.31	0.25	0.25	0.18	0.29	0.36	0.45	0.00
14	RealWear HMT-1 (2017)	0	0.83	1.00	0.25	0.13	0.20	0.25	0.12	0.20	0.00
15	Glassup F4 (2017)	0	0.58	0.31	0.13	0.13	0.24	0.28	0.18	0.23	0.00
16	ODG R-9 (Worrel 2017)	0	0.42	0.50	0.75	1.00	0.08	0.63	0.25	0.28	0.00

$45/60 = 0.75$.

Table 1 summarizes the parameters and the corresponding weighting coefficients to the parameters. The last column of Table 1 lists the total evaluation score of each AR device in descending order. The authors selected the Microsoft HoloLens 2 platform to design the TMM application. Besides the highest score, the Microsoft HoloLens2 is an HMD controlled by air tapping gestures that enable the user to interact with holographic information without the need for external handheld devices.

4. AR software design

As previously stated, the primary functions of TMM are time machine and measure. The time machine function enables inspectors to observe and compare the current environment to virtual environments from the past. The measure function allows the measurement of deformations over time. The following sections describe the development and use of these two functions in detail.

4.1 Time machine function

The time machine function enables a 3D representation of the past to be saved and restored to be displayed simultaneously with the immediate environment. The AR device can track users' positions in space using the spatial mapping function to place stable and accurate holograms despite the users' movement. Hence, the AR device can recognize proper positioning even from different perspectives. The following procedure is to fulfill the time machine function. The spatial mapping of the real environment is defined at time *t* as

$$\{\mathbf{I}_n\}_t = (x, y, z, t)^T, n \in [1, N] \quad (2)$$

where n represents the n^{th} mesh element of the real environment; N is the total number of the mesh elements in this environment; $\mathbf{I}_n$ is the spatial mapping consisting of n mesh elements; t represents the timestamp of the spatial mapping; and (x, y, z) are the three-dimensional position coordinates.

Fig. 2 explains the time machine function with the

(a) Real image $\{\mathbf{I}_n\}_{t_1}$ (b) Real image $\{\mathbf{I}_n\}_{t_2}$ and virtual image $\{\mathbf{I}_n\}_{t_1}$

Fig. 2 Illustration of the time machine function

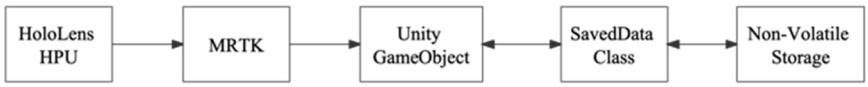

Fig. 3 Time machine function components

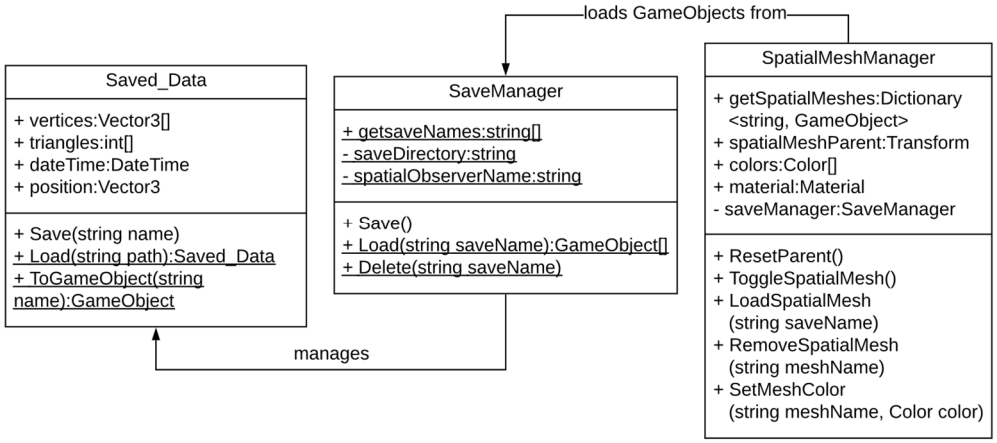

Fig. 4 Time machine function flowchart

movement of a lamp. The lamp labeled with a red frame is a real object (i.e., a physical lamp in the room), and the one with a blue frame is virtual (i.e., simulated meshes of a lamp). In Fig. 2(a), the environment is mapped, and the meshes of the lamp in the position P_1 are saved as $\{\mathbf{I}_n\}_{t_1}$. In Fig. 2(b), the lamp has been moved from position P_1 to P_2, and $\{\mathbf{I}_n\}_{t_1}$ is restored, i.e., the virtual lamp at the position P_1. In summary, with the time machine function, the users can simultaneously observe the saved images from the past and the actual object in the environment.

The time machine function leverages Microsoft's Mixed Reality Toolkit (MRTK 2020) mesh observer to add a collection of meshes. The meshes represent the geometry of the nearby real-world environment in the Unity scene. The MRTK mesh observer gets real-time environment data from the HoloLens Holographic Processing Unit (HPU). Fig. 3 summarizes the saving and loading procedure in the TMM. Fig. 4 shows a more detailed description of the time machine design frame.

The mesh vertices, triangles, and time are saved to the non-volatile memory as an XML file for later access. This process is performed by a custom class to make a deep copy of the vertices and triangles of the meshes from the MRTK mesh observer. A deep copy is required because the mesh data is read-only, and Unity components cannot be directly serialized. The custom class then adds a timestamp to the deep copied meshes, copies the mesh positions relative to the observer, and serializes the System.Xml.Serialization component (Joshi 2017) from the .NET Runtime Library.

To load a saved mesh, a Unity GameObject is created with four components attached, i.e., MeshFilter, MeshRenderer, MeshCollider, and TimeMachineData. The MeshFilter, MeshRenderer, and MeshCollider are components provided by the Unity game engine to enable the rendering and collision of meshes. The TimeMachineData is a custom-defined component. The saved XML file is then deserialized into an int array that defines the mesh triangles, a 3-point vector array that defines the mesh vertices, and a timestamp. The triangles and vertices are then copied to the MeshFilter; the timestamp is assigned to the TimeMachineData, and the new GameObject's position is set to the saved position. When restoring the saved mesh, the HoloLens sensors automatically map and recognize the nearby real-world environment to accurately place the saved mesh based on the position of the HoloLens wearer. A saved mesh can also be placed in a different environment.

4.2 Measure function

The 3D transformation from time t_1 to t_2 consists of a 3D rotation $\Delta\mathbf{I}_{\mathrm{Rot}}$ and a 3D translation $\Delta\mathbf{I}_{\mathrm{Tra}}$. Combining $\Delta\mathbf{I}_{\mathrm{Rot}}$ and $\Delta\mathbf{I}_{\mathrm{Tra}}$ in a transformation matrix $\Delta\mathbf{I}$, then $\Delta\mathbf{I}$ is a rigid motion.

$$\Delta\mathbf{I} = \begin{bmatrix} \Delta\mathbf{I}_{\mathrm{Rot}} & \Delta\mathbf{I}_{\mathrm{Tra}} \\ \mathbf{0} & \mathbf{1} \end{bmatrix} \tag{3}$$

$$\{\mathbf{I}_n\}_{t_2} = \Delta\mathbf{I}_{t_1 \to t_2}\{\mathbf{I}_n\}_{t_1}, n \in [1, N] \tag{4}$$

The measure function is to measure $\Delta\mathbf{I}$, especially $\Delta\mathbf{I}_{\mathrm{Tra}}$, as shown in Eq. (3). The dimension of $\Delta\mathbf{I}_{\mathrm{Tra}}$ is 2Nx2N, where N represents the number of nodes. The programming of the measure function is based on the spatial mapping that recognizes the surrounding environment. The authors use a script consisting of the Measure Manager, Input Manager, and Spatial Mapping components to conduct the measurement, as shown in Fig. 5. The Measure Manager manages all the measurements in the Unity platform, and the Input Manager handles the input according to the users' sight and gesture. Fig. 6 shows a more detailed description of the measure function design frame.

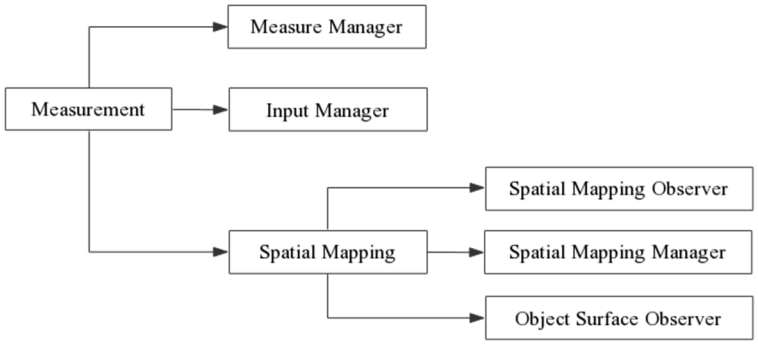

Fig. 5 Measure function components

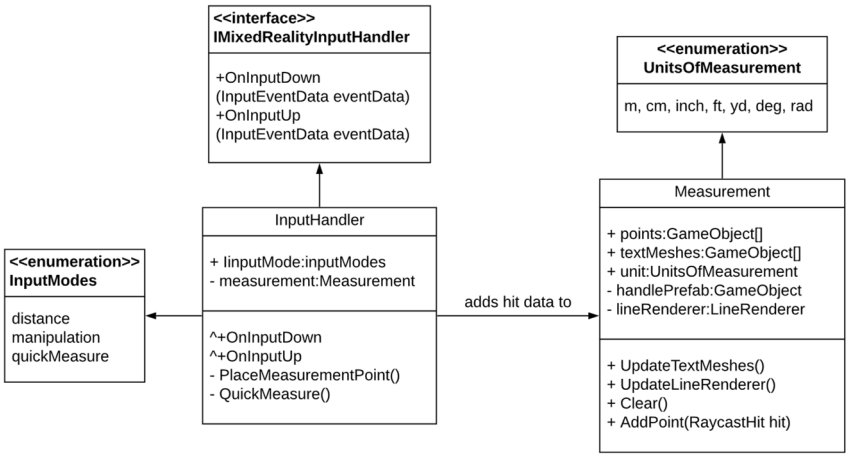

Fig. 6 Measure function flowchart

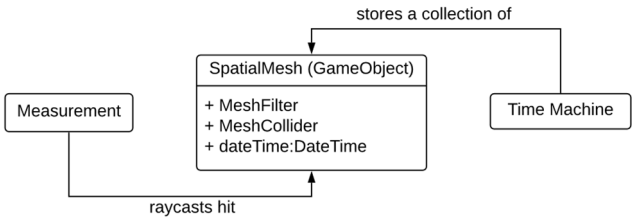

Fig. 7 Measurement over time flowchart

The Spatial Mapping component consists of three scripts, Spatial Mapping Observer, Spatial Mapping Manager, and Object Surface Observer. The Spatial Mapping Observer script is to manage the Surface Observer component to conduct an environmental scan. The Object Surface Observer component scans the surrounding environment and loads the mesh holograms. The Spatial Mapping Manager script has four functions: (i) restore the Surface Observer component, (ii) store the mesh data obtained by the Spatial Mapping component, (iii) shut down the Surface Observer component, and (iv) update the Spatial Mapping component in real-time while TMM is loading the mesh data.

4.3 Measurement over time

The authors combined the two primary functions of the TMM, time machine and measure, by leveraging Unity's layer system and a custom class to store time information on loaded GameObjects. Full meshes are assigned to the same layer as the meshes from the Spatial Observer component so that ray casts from the InputHandler (Fig. 6) collide with the MeshCollider component. The InputHandler component checks the TimeMachineData component on any hit objects, allowing measurement over time by comparing the saved time of the hit meshes. If the InputHandler does not find a TimeMachineData component, it uses the current time to compare with the other meshes. Fig. 7 shows a more detailed description of the measurement over time function design frame.

To demonstrate the measurement function and examine the accuracy and efficiency of the AR device's sensors, the authors first test the measure function of the application in comparison to traditional measurement methods. The experiment is designed to test (a) a small-scale feature that requires high precision and (b) a larger scale feature the

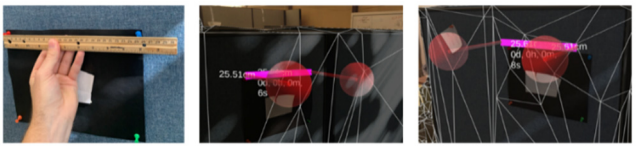

Fig. 8 Traditional measurement of feature versus measurement with the AR measure function, taken from an angle right to left and left to right respectively

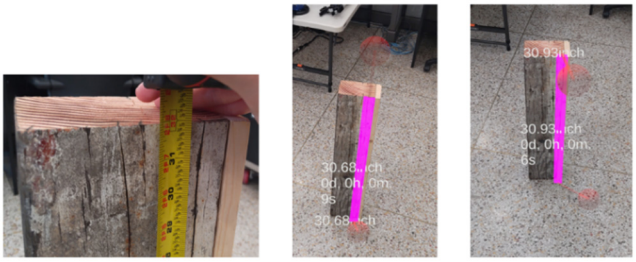

Fig. 9 Traditional measurement of feature versus measurement with the AR measure function, taken from top to bottom and bottom to top respectively

requires lower precision and in conjunction (c) the accuracy of multiple measurements taken from different angles with different units. Feature (a) is a board pinned with four tacks arranged in a rectangular pattern where feature (b) is a rectangular section of wood. To weigh the results of the measurements, the authors compare feature (a) to a ruler and feature (b) to a tape measurer, where (a) is taken in centimeters and (b) is taken in inches. The results of this demonstration are reported and shown in Figs. 8 and 9. The error is reported with respect to the traditional method and to the separate AR measurements and the source of error is considered.

The error in measurements performed on the tack board is 0.039% taken from the left angle and 0.43% taken from the right compared to the 25.5 cm ruler measurement. A ruler is used as the ground-truth measurement to compare the TMM measure function to a common tool used in inspections. On the larger scale, the measurements resulted in a 3.75% error (top to bottom) and 2.96% (bottom to top) compared to the ground-truth measurement of 31.87 inches with a tape measurer.

The results confirm that small measurements are more accurate than longer distances, which is a positive result as small movements are more pertinent to real-time changes in inspections.

Section 6 includes a demonstration of the combined functions time machine and measure with an experiment to test the combination of the functions.

5. Human-device interface

This section presents the human-device interface and illustrates the functions of different modules. Fig. 10 shows the full view of the TMM human-device interface. The two modules in the TMM interface are the time machine menu

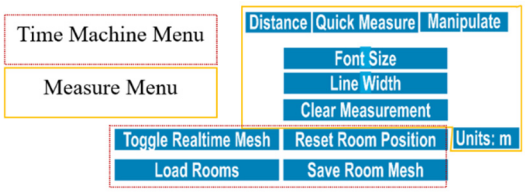

Fig. 10 The TMM human-device interface

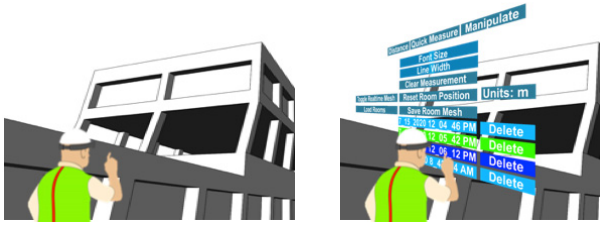

(a) Spatial mapping of the real environment

(b) TMM interface in an implementation

Fig. 11 Measuring movements across time

and the measure menu. These correspond to the time machine and measure functions. The interface is developed with human factors considered where each button is clearly labeled, and the functions work simply for an inexperienced AR user. Fig. 11 is a schematic diagram illustrating the interface during the implementation. The following subsections show a detailed explanation of the functions and instructions of each module.

5.1 Interface menus

The measure menu contains the following keys: Distance, Quick Measure, Manipulate, Font Size, Line Width, Clear Measurement, and Units. The time machine menu includes the following functions: Toggle Real-time Mesh, Reset Room Position, Load Rooms, and Save Room Mesh. Table 2 summarizes the functions of each key in detail. The authors name the keys in the interface according to their operations and show them directly in the menu to decrease cognition load.

5.2 Control gestures

The user interfaces with the menus and keys of the TMM using hand gestures and their gaze following this sequence: (i) user gazes at the hologram meant to be clicked; (ii) user points the index finger straight up toward the ceiling; and (iii) user air taps the key intended to be accessed by first lowering the finger and then quickly raising it. Fig. 12 summarizes the control gesture of the air tap.

To conduct a measurement, the user first points to a node as the starting point with the index finger of their right hand then points to another node with a different timestamp endpoint (i.e., from a saved and loaded image). The interface then shows the distance between the start and endpoints automatically.

Table 2 The function of each key in the interface

#	*Menu*	*Key*	*Function*
1	Time Machine	Toggle Real-time Mesh	Scan the surroundings
2		Reset Room Position	Reset the environment and re-scan the surroundings
3		Load Rooms	load a pre-scanned environment
4		Save Room Mesh	Save the mapping of the current environment
5	Measure	Distance	Measure distance between two points
6		Quick Measure	Measure with default settings
7		Manipulate	Downsize the virtual environments
8		Font Size	Modify the measurement font size
9		Line Width	Modify the measurement line width
10		Clear Measurement	Clear all measurements
11		Units	Show the measurement units

(a) Front image (b) Profile image

Fig. 12 Air tap gestures to control the TMM by user

5.3 Color

The current version of the TMM can simultaneously save a maximum of six environment meshes with different timestamps. Therefore, there could be a maximum of six virtual environments displayed overlapping onto the reality at a given time. The saved meshes with different timestamps are shown in different colors to decrease cognition load for the users. An inspection site can have low visibility. Therefore, the authors select opposite colors with high saturation for meshes in a sequence. Two contiguous meshes are restored with opposite colors according to the color wheel to generate high contrast and improve the visualizations of the variations in time (Cohen-Or *et al.* 2006). With the contrasting colors selected, the measurement procedure between different meshes will be less time-consuming. The colors implemented in the TMM interface are cyan, orange, lime, red, blue, and magenta.

5.4 Special functionalities

Three functionalities are designed in the interface to help the users implement the TMM application. These are timestamp, downsizing, and automatic font scaling. The following subsections provide detailed explanations of these three functionalities.

5.4.1 Timestamp

Displaying timestamps helps distinguish how the environment has been changing over time. Without the timestamps, it would be difficult for the users to tell the measurement duration and it is valuable to document the time and date that prior captures were taken. Timestamps of saved meshes are automatically loaded and displayed on the TMM interface, where each key has a timestamp and color that matches the corresponding mesh. The demonstration of the TMM section shows examples of the timestamp feature.

5.4.2 Downsizing

The downsizing feature of the application allows the user to manipulate the size and angle of one capture or overlaid captures. This feature is necessary for easy viewing of the saved environment, enabling the users to inspect the surroundings quickly. It also allows the users to manipulate the view to take measurements and draw conclusions more quickly. Users can deploy the downsizing feature by air tapping the 'Manipulate' key (right upper corner in Fig. 10) and then pinching with both hands. Users can move both hands closer to downsize the Fig. and change either hand's position to alter the angle. The demonstration of the TMM section shows an example of the downsizing feature.

5.4.3 Automatic font scaling

Both the font size and line width of the measurement results can be adjusted automatically or manually. Users can alter the font size and line width by the sliders on the 'Font Size' and 'Line Width' keys, as shown in Fig. 10. The measurement text is rendered in 3D space and scaled relative to the user's distance to maintain font readability with different lengths.

6. TMM experiment

The research team tested the new application in a fundamental scenario to better demonstrate its value in an engineering context, as well as to be able to extrapolate the first validation in various domains of engineering across disciplines. Additionally, the research team met with leaders of an emergency office management in a large city in the US. For innovation and practical development of AR solutions, experts in emergency rescue prefer to first test the

application indoors in fundamental scenarios to better understand its capabilities to their teams and enable them to provide input before more complex scenarios. The researchers followed this sequence and enabled them to first test the TMM in simple scenarios and also collected their recommendation for complex scenarios future considerations, including the temperature time machine recommendation from their team. Their input is added at the end of the paper, along with the limitations to be explored in the future. This experiment is to verify the accuracy of the measurement over time function and show its convenience and efficiency over the traditional measuring method.

6.1 Experiment description

The authors conducted two experiments to verify the reliability of the TMM in comparison with traditional measurement methods. To this end, one piece of furniture, a cube storage unit, was moved and the movement was measured by both the traditional tape measure and the TMM. The same was done with a metal shelf, meant to simulate a real-time change that could lead to the fall of a structure that endangers the inspector. The traditional method is unable to remember the original location for the experiment with the storage unit, so the authors marked the floor with the original and final position (Fig. 13(a)). The initial and final positions of the metal shelf are measured by a ruler with reference to the wall that is 1 cm from the shelf. The tape measurer and ruler are used to comparing the result obtained by TMM to a traditional approach of measurement, where it is expected that the error induced by the traditional method is close to zero.

6.2 Measurements

The authors validated the TMM by conducting two measurements simultaneously and comparing them. The two different measurement approaches are described herein, for comparison purposes:

1. Figs. 13(b) and (c) show the traditional tape measurement sequence: first, the authors marked the starting position of the object that would serve as a reference about its past position; then, after the movement, a mark was added that would serve as the present position of interest; finally, the authors used a tape measure to measure the distance between the marks representing past and present positions, which was the movement across time. Figs. 13(e) and (f) show the movement of the metal shelf and the measurement with ruler with respect to the initial position 1 cm from the wall.
2. Figs. 13(d) and (h) shows the measurement using the TMM: the user can collect the change on position without marks on the ground or any form of marking initial position. The TMM overlapped the virtual objects from both the past and the present time of the movement simultaneously, and the user measured the movement of the object across time. Additionally, the user can measure more than one movement across time, enabling multiple comparisons across time with small effort. This also means that while the inspector is only paying attention to one area, the TMM continues to map the nearby surroundings and can potentially lead to the discovery of movements that the inspector failed to observe.

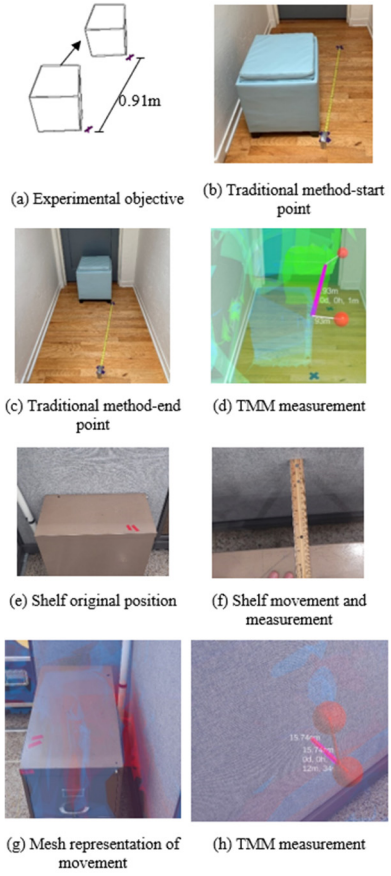

Fig. 13 TMM verification experiment

6.3 Experimental results

The measuring result by the traditional method for the storage unit is 0.91 m, and by the TMM is 0.93 m. The difference in measurements is 2.20%. For the metal shelf, the traditional measurement gave exactly 16 cm versus 15.74 cm by TMM. The measuring difference for the metal shelf is 1.62%. The accuracy of the measurements will depend on how precisely the characteristic points of the objects are modeled, for instance, the corner points of a box object, because the characteristic points are where the inspector chooses to measure.

The measuring difference is induced by (i) the spatial mesh precision; and (ii) the user's air tapping accuracy. Inspectors can more accurately place pins for smaller movements, and inspectors are more interested in small movements as it is more common to observe small changes in the built environment. The traditional method takes approximately 5 min to set the markers and conduct the measurement with no awareness of the initial position of the object. In comparison, the TMM takes less than 1 min for

an experienced AR user. Setting markers is inconvenient, time-consuming, sometimes even not applicable during an inspection, and inspectors may not know the original position of a structure or object in the built environment.

7. TMM demonstration experiment

This demonstration simulates an environment in which inspectors can observe and measure changes across time. This demonstration shows the features of the TMM application by executing the same steps as an inspection task: capturing and overlaying separate environments to measure the changes between captures over time. The authors conduct one demonstration experiment in a residential house to test the TMM in a realistic scenario where results can have the highest impact for inspections in the future.

7.1 Experiment procedure

There are seven steps in the demonstration:

1. Nominate and save the initial environment when the inspectors enter the site to verify the timestamp function.
2. Move the object to simulate the environmental change.
3. Restore the saved initial environment to verify the time machine function.
4. Measure over time using the measure function and save the current environment, verifying the measurement over time function.
5. Move the object again to simulate a continuous environmental change.
6. Restore the saved images and measure over time to verify the robustness of the measurement over time function.
7. Manipulate virtual images to verify the downsizing function (done only for the storage unit).

7.2 Experiment results

The following are the demonstration results:

(a) The authors nominate the time of the initial environment as t_1. The environment at time t_1 is saved with a timestamp and appointed as $\{\mathbf{I}_n\}_{t_1}$ (cyan color), as shown in Fig. 14(a).

(b) The cube storage is moved from the initial location to a new location during the time t_1 to t_2. The environment at time t_2 is saved with a timestamp and nominated as $\{\mathbf{I}_n\}_{t_2}$ (lime color).

(c) At time t_2, the saved $\{\mathbf{I}_n\}_{t_1}$ is restored as a virtual image. Both the real $\{\mathbf{I}_n\}_{t_2}$ and virtual $\{\mathbf{I}_n\}_{t_1}$ are shown to the user at the same time, as shown in Fig. 14(b). The users can maneuver the color-coded environments to observe the cube storage movement and verify the capture capabilities of the TMM.

(d) At time t_2, measure $\Delta\mathbf{I}_{t_1\to t_2}$ by air tapping the cube storage in each capture. The interface will then show the distance between points pinned at two desired locations with the elapsed time between the captures. The moving distance in step (b) is 0.87m, as shown in Fig. 14(c).

(e) Save the environment at time t_2 it as $\{\mathbf{I}_n\}_{t_2}$ (lime color). Furthermore, move the cube storage again, as shown in Fig. 14(d).

(f) At time t_3, restore both $\{\mathbf{I}_n\}_{t_1}$ and $\{\mathbf{I}_n\}_{t_2}$ as virtual images. Measure $\Delta\mathbf{I}_{t_1\to t_3}$. The total moving distance is 1.8 m, as shown in Fig. 14(e).

(g) The authors verify the downsizing feature by shrinking the three collaborative environments. With the downsizing function, users can conveniently obtain a whole picture of the surroundings in which they are standing. Users can observe the relative position of the object in the environment. Additionally, the downsizing function can clearly show the observed object's movement trail, shown as the red line in Fig. 14(f).

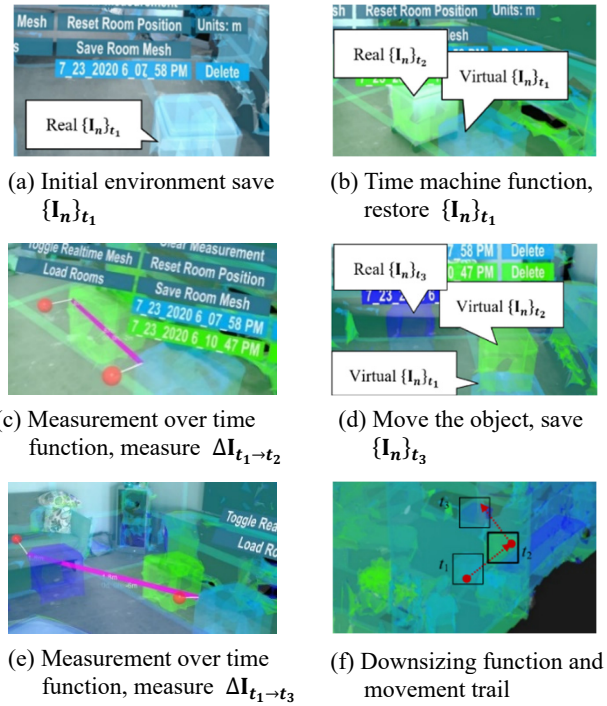

(a) Initial environment save $\{\mathbf{I}_n\}_{t_1}$

(b) Time machine function, restore $\{\mathbf{I}_n\}_{t_1}$

(c) Measurement over time function, measure $\Delta\mathbf{I}_{t_1\to t_2}$

(d) Move the object, save $\{\mathbf{I}_n\}_{t_3}$

(e) Measurement over time function, measure $\Delta\mathbf{I}_{t_1\to t_3}$

(f) Downsizing function and movement trail

Fig. 14 Demonstration of TMM implementation

7.3 Limitations

High luminance, high temperature and moderate impacts inherent to normal outdoor environments can be a challenge to most AR devices:

(a) HoloLens uses visible light to track the user's location and the surroundings, hence requiring a steady 500-1000 lux luminance for best performance. If the environment is too bright, the cameras can get saturated, and nothing is seen. If the environment is too dark, the cameras cannot pick up enough information, and nothing is seen (Microsoft 2019). The luminance of 500 lux is the light of a typical indoor environment, e.g., offices, groceries, and laboratories. The luminance of 1000

lux is the light of a bright indoor environment, e.g., detailed mechanical workshops and operation theatres.

(b) HoloLens operates with the best performance in environments within the temperature range of 10-27°C (50-81°F) and the humidity range of 8%-90% relative humidity. In the researchers' experiments, HoloLens can operate in environments out of these ranges. However, implementations out of the recommended range may lead to the device shutting down, a shorter battery life, or permanent device damage.

(c) The research team has tested the application outdoors and in various environments and, by error, dropped the device three feet from the ground, resulting in the device not being reparable. The research team recommends reinforcing the device against small impacts and/or accidental drops, which are inherent to be practical for professionals in any type of field implementation.

8. Conclusions

SHM inspectors can benefit from a convenient method to observe and measure both real-time changes and changes over extended periods of time in the built environment to ensure safety and track the damage pattern. Inspired by input from first responders for inspection priorities in buildings after disasters, the authors developed an AR application to measure the displacements and other movements in the immediate environment over time. TMM has two primary functions, time machine and measure. With the time machine function, users can save and restore the surroundings as virtual meshes. The virtual meshes can then be displayed overlapping the real environment or multiple virtual meshes. With the measure function, the users can measure the distance of changes between the virtual and real meshes. Consequently, TMM enables inspectors to measure environmental movements over time.

Besides the two primary functions, the authors also design some practical functionalities for the TMM. First, the saved environments are stamped with different saturate and opposite colors to be easily distinguished. Then, the measurement fonts and line width can be automatically adjusted to minimize eye strain. Next, the virtual environment can be downsized for easy viewing and an intuitive perspective of the entire scan. Users can control the completed TMM by gaze and hand gestures, freeing both hands for inspection tasks. Finally, the authors designed the human-device interface to be instinctively controlled to minimize cognitive load.

The future work of this research includes the following:

(a) Voice input and eye-ball tracking will be used with the TMM application, allowing the user to perform actions in the AR application with their gaze and voice.

(b) TMM will be improved to make it more suitable for more complex environments and challenging conditions, including high luminescence, high temperature, and small accidental impacts.

Additionally, based on the research conducted in this pilot study, it is of critical value to share early prototypes with emergency officers and to listen to their recommendations regarding the practical limitations of AR prior to testing them in complex scenarios. Meeting with the industry early in the development phase enables researchers to engage them with the development from the start as well as to receive critical input early, and to reflect their positive input and constructive feedback so that both research and technology transfer can be developed together. Sharing early prototypes with the industry can contextualize its potential as a valuable reference for future research and innovation that combines scholarship and implementation together.

Acknowledgments

The financial support for this research is provided in part by the Air Force Research Laboratory (AFRL, Grant number FA9453-18-2-0022), and the New Mexico Consortium (NMC, Grant number 2RNA6.) The authors appreciate the discussion and feedback from the Department of Emergency Management in the City of Albuquerque. The conclusions of this research represent solely those of the authors.

References

Burachek, V., Khomushko, D., Tereshchuk, O., Kryachok, S. and Belenok, V. (2022), "Analysis of development tendencies of metrological technologies to control rangefinders of an electronic distance measurement instruments", *Adv. Geodesy Geoinform.*, **71**(1), e13. https://doi.org/10.24425/gac.2022.140504

Carbotte, K. (2018), "Kopin's Golden-i Infinity is a Wearable Display for Smartphones, Tablets". https://www.tomshardware.com/news/kopin-golden-i-infinity-smart-display,37138.html

Cohen-Or, D., Sorkine, O., Gal, R., Leyvand, T. and Xu, Y.Q. (2006), "Color harmonization", In: *ACM SIGGRAPH 2006 Papers*, pp. 624-630. https://doi.org/10.1145/1179352.1141933

DAQRI Smart Glasses (2017). https://daqri.com/products/smart-glasses/

Diao, F., Wang, R., Xiong, X. and Liu, C. (2021), "Overlapped postseismic deformation caused by afterslip and viscoelastic relaxation following the 2015 Mw 7.8 Gorkha (Nepal) earthquake", *J. Geophys. Res.: Solid Earth*, **126**(3). https://doi.org/10.1029/2020JB020378

Epson (2017a), Adjustable, Highly Transparent Smart Glasses for Multi-User Applications. https://epson.com/For-Work/Wearables/Smart-Glasses/Moverio-BT-350-Smart-Glasses/p/V11H837020

Epson (2017b), Durable Smart Headset Built for Industrial, Hands-Free Applications. https://epson.com/For-Work/Wearables/Smart-Glasses/Moverio-Pro-BT-2200-Smart-Headset/p/V11H853020#

Everysight Raptor (2017). https://everysight.com/

Glass Enterprise Edition 2 Tech Specs (2019). https://www.google.com/glass/tech-specs/

Glassup F4 (2017). https://www.glassup.com/en/f4/

He, K., Xu, C. and Wen, Y. (2022), "Coseismic and early post-seismic deformations due to the 2019 earthquake sequence in Ridgecrest, California", *Geophys. J. Int.*, **230**(2), 957-975. https://doi.org/10.1093/GJI/GGAC103

Holmgren, M., Johansson, D. and Andersson, K. (2014), "A web-based time machine with augmented reality", In: *IEEE Conference on Local Computer Networks*.

Jin, Z. and Fialko, Y. (2021), "Coseismic and early postseismic deformation due to the 2021 M7. 4 Maduo (China) earthquake", *Geophysical Research Letters*, **48**(21), e2021GL095213. https://doi.org/10.1029/2021GL095213

Joshi, B. (2017), "XML Serialization", In: Beginning XML with C# 7, pp. 211-237, Berkeley, CA, USA. https://doi.org/10.1007/978-1-4842-3105-0_8

Kamat, V.R. and El-Tawil, S. (2005), "Rapid post-disaster evaluation of building damage using augmented situational visualization", In: *Construction Research Congress 2005: Broadening Perspectives*, pp. 1-10.

Kamat, V.R. and El-Tawil, S. (2007), "Evaluation of augmented reality for rapid assessment of earthquake-induced building damage", *J. Comput. Civil Eng.*, **21**(5), 303-310. https://doi.org/10.1061/(ASCE)0887-3801(2007)21:5(303)

Lim, C.H., Zhang, L. and Amaludin, A.E. (2021), "Topographic Survey and Modelling Using Photogrammetry: A Comparison against Electronic Distance Measurement (EDM) Method", *ASM Sci. J.*, **16**. https://doi.org/10.32802/asmscj.2021.720

Lu, L., Duan, Y.F., Spencer Jr, B.F., Lu, X. and Zhou, Y. (2017), "Inertial mass damper for mitigating cable vibration", *Struct. Control Health Monitor.*, **24**(10), e1986. https://doi.org/10.1002/stc.1986

Magic Leap 1 (2018). https://www.magicleap.com/en-us/magic-leap-1

Mandler, E., Pintori, F., Gualandi, A., Anderlini, L., Serpelloni, E. and Belardinelli, M.E. (2021), "Post-Seismic Deformation Related to the 2016 Central Italy Seismic Sequence From GPS Displacement Time-Series", *J. Geophys. Res.: Solid Earth*, **126**(9), e2021JB022200. https://doi.org/10.1029/2021JB022200

Microsoft (2019), Environment Considerations for HoloLens. https://rb.gy/kb5xay

Realwear (2017), HMT-1: The World's Leading Hands-Free Remote Collaboration Tool. https://www.realwear.com/products/hmt-1/

Realwear (2018), HMT-1Z1: The World's Only Intrinsically Safe Hands-Free Remote Collaboration Tool. https://www.realwear.com/products/hmt-1z1/

Rick, J.W. (2018), "Total Station", In: *The Encyclopedia of Archaeological Sciences*, pp. 1-3. https://doi.org/10.1002/9781119188230.saseas0205

Sahu, R.K. (2021), "A review on application of laser tracker in precision positioning metrology of particle accelerators", *Precision Eng.*, **71**, 232-249. https://doi.org/10.1016/j.precisioneng.2021.03.015

Shan, J., Ouyang, Y., Yuan, H. and Shi, W. (2016), "Seismic data-driven identification of linear models for building structures using performance and stabilizing objectives", *Comput.-Aided Civil Infrastr. Eng.*, **31**(11), 846-870. https://doi.org/10.1111/mice.12227

Okada, S. and Takai, N. (2000), "Classifications of structural types and damage patterns of buildings for earthquake field investigation", *Proceedings of the 12th World Conference on Earthquake Engineering*, Vol. 30.

Solos Smartglasses (2018).

Sony, S., Laventure, S. and Sadhu, A. (2019), "A literature review of next-generation smart sensing technology in structural health monitoring", *Struct. Control Health Monitor.*, **26**(3), e2321. https://doi.org/10.1002/STC.2321

The Mixed Reality Toolkit (MRTK) (2020). https://docs.microsoft.com/en-us/windows/mixed-reality/mrtk-unity/?view=mrtkunity-2021-05

ThirdEye Gen X2 Mixed Reality Smart Glasses (2019). https://thirdeyegen.com/x2-smart-glasses

Toshiba DynaEdge AR100 Head Mounted Display (2018). https://us.dynabook.com/smartglasses/products/index.html

Vuzix M400 Augmented Reality (AR) Smart Glasses (2020). https://www.vuzix.com/products/m400-smart-glasses

Worrel, J. (2017), "ODG Unveils R8 and R9 Smartglasses at CES". https://www.fudzilla.com/news/42622-odg-unveils-r8-and-r9-smartglasses-at-ces

Xu, J., Doyle, D. and Moreu, F. (2022), "State of the Art of Augmented Reality (AR) Capabilities for Civil Infrastructure Applications (in Submission)", Engineering Reports. arXiv preprint arXiv:2110.08698

Yekrangnia, M., Torabizadeh, A. and Brzev, S. (2021), "Post-Earthquake Damage Assessment of Buildings: Comprehensive Experimentally-Based Maximum Drift Ratio Predictive Model Based on Residual Drift Ratio", *J. Earthq. Eng.*, 1-45. https://doi.org/10.1080/13632469.2021.1961934

You, T., Wang, W., Fang, C. and Chen, Y. (2022), "Rapid probabilistic loss assessment of buildings based on post-earthquake structural deformation conditions", *J. Build. Eng.*, **45**, p. 103629. https://doi.org/10.1016/j.jobe.2021.103629

Zoellner, M., Pagani, A., Pastarmov, Y., Wuest, H. and Stricker, D. (2008), "Reality Filtering: A Visual Time Machine in Augmented Reality", In: *The 9th International Symposium on Virtual Reality, Archaeology and Cultural Heritage*, pp. 71-77. https://doi.org/10.2312/VAST/VAST08/071-077